
Efficient Image Deblurring Networks based on Diffusion Models

Kang Chen, Yuanjie Liu*

College of Information and Electrical Engineering
China Agricultural University

Abstract

This article presents a sliding window model for defocus deblurring, named Swintormer, which achieves the best performance to date with remarkably low memory usage. This method utilizes a diffusion model to generate latent prior features, aiding in the restoration of more detailed images. Additionally, by adapting the sliding window strategy, it incorporates specialized Transformer blocks to enhance inference efficiency. The adoption of this new approach has led to a substantial reduction in Multiply-Accumulate Operations (MACs) per iteration, drastically cutting down memory requirements. In comparison to the currently leading GRL method, our Swintormer model significantly reduces the computational load that must depend on memory capacity, from 140.35 GMACs to 8.02 GMACs, while improving the Peak Signal-to-Noise Ratio (PSNR) for defocus deblurring from 27.04 dB to 27.07 dB. This innovative technique enables the processing of higher resolution images on memory-limited devices, vastly broadening potential application scenarios. The article wraps up with an ablation study, offering a comprehensive examination of how each network module contributes to the final performance.

1 Introduction

Image deblurring is a classic task in low-level computer vision, which aims to restore the image from a degraded input and has a wide range of application scenarios. Existing networks based on supervised deep learning regression methods such as Restormer [81], GRL [41] show strong capabilities for image deblurring tasks. However, such supervised algorithms invariably demand a considerable volume of labeled data to effectively train regression models. Data annotation is labor-intensive and often necessitates domain expertise, thereby resulting in elevated costs. Conversely, unsupervised learning methods [39, 59, 26] obviate the need for labeled data, rendering them particularly well-suited for large-scale datasets. Nevertheless, acquiring extensive data can pose challenges in certain tasks, and in such contexts, unsupervised methods may not prove to be as efficacious as supervised algorithms. Another important issue is the generalization ability. The current deblurring algorithms [1, 66, 38, 78] often suffer severe performance degradation when confronted with varying data distributions across different scenarios.

In recent years, attention mechanisms [63, 1, 38, 66] have demonstrated their effectiveness in enhancing the fitting capability of deep learning regression models. Convolution operations, which are often used to implement attention mechanisms, provide local connectivity and translation invariance. While convolution operations enhance efficiency and generalization, the convolution operator's receptive field is restricted, impeding its ability to model long-range pixel dependencies. As a result, Transformer-based algorithms utilizing the self-attention (SA) mechanism [74, 77, 83, 17] were introduced to address this challenge. Although SA is highly effective in capturing long-range pixel interactions, its complexity grows quadratically with spatial resolution. This makes it impractical to

*Corresponding author.

apply to high resolution images, which is often the case in image deblurring. Recently, there have been some attempts to customize the attention mechanism for image deblurring tasks [42, 78, 81]. To reduce the computational loads, these methods either apply SA on small 8×8 spatial windows around each pixel [42, 78, 41], or substitute the fully connected layer in the attention mechanism with a more efficient convolution operation [81] with sparsity.

In addition to regression-based methods, leveraging deep generative models presents a promising approach for enhancing image deblurring tasks. Noteworthy deep generative models such as Generative Adversarial Networks (GANs) [23, 29], Variational Auto-Encoding model [35] and Diffusion models (DM) [26] have demonstrated remarkable performance in image synthesis and super-resolution tasks. Moreover, these generative models are typically trained using unsupervised algorithms, obviating the need for labeled data. In contrast, many existing supervised tasks rely on image datasets containing only a few hundred images, thereby providing limited image information. However, generative models exhibit the ability to learn intricate distributions from extensive datasets, such as ImageNet [62], CIFAR [69], and COCO [47], which extends beyond the constraints of current labeled datasets. Nevertheless, it’s important to note that generative models, especially state-of-the-art Diffusion models (DM), often necessitate more computational resources compared to regression models. With billions of parameters, these models significantly increase computational overhead.

To address this limitation, we explored the subtle modeling capability of DM by directly using Robin’s pre-trained super-resolution DM [59] to produce high-resolution images on the deblurring dataset DPDD [1]. Remarkably, even after the inevitable downsampling to match the input image size, as shown in Table 1, we observe a substantial performance enhancement of 0.24dB for single pixel defocus deblurring. This attests to DM’s proficiency in deblurring tasks. DM’s ability of implicit modelling benefits from a surfeit of training data with diverse images, improving its understanding of image content and structure for detail recovery in various conditions. DM uses maximum likelihood estimation to find parameters best fitting the training data distribution:

$$\nabla_{\theta} \|\epsilon - \epsilon_{\theta}(z_t, t)\|_2^2. \quad (1)$$

where z represents prior features, $t \in [1, T]$ is a random time-step and $\epsilon \sim \mathcal{N}(\mathbf{0}, \mathbf{I})$ denotes sampled noise. The unique training strategy has given DM a significant advantage in its ability to generalize across various conditions. However, it is not well-suited to supervised learning tasks like classification or regression, as DM’s main focus is on modeling the data distribution rather than predicting specific target values. Consequently, we are now undertaking an exploration of fine-tuning and adjustments rooted in the DM paradigm, in a collaborative effort to improve its performance across a range of tasks.

In addition to the aforementioned challenges, another often overlooked issue is the inconsistency between training and inference. Take Restormer [81] for example, where the training process involves a tensor input of $128 \times 128 \times 3 \times 8$, yet during inference, a $1680 \times 1120 \times 3 \times 1$ tensor is used. This discrepancy between training and inference can detrimentally affect a model’s performance. A recent approach, TLC [12], addresses this issue by substituting global operations (like global average pooling) with local operations at inference time. However, this module-swapping technique doesn’t universally apply to all models. To tackle this challenge, we propose a sliding window-based approach aimed at addressing this inconsistency.

Based on the above analysis, we propose a novel approach for image deblurring that is capable of fusing more image information and also applicable for large images. Firstly, we use a DM model that loads the best pre-trained parameters to generate latent image features based on existing supervised dataset. We then proceed to train the deblurring network by inputting the latent image features and the label dataset simultaneously. Lastly, we present a broader approach to addressing the inconsistency in the distribution of global information during training and inference. The main contributions of this work are summarized below:

- We propose Swintormer, a Sliding Window Transformer for multi-scale representation learning on high-resolution images. It incorporates latent image feature fusion to effectively deblur images.
- We propose a novel training scheme that utilizes DM to generate image features conditionally, enabling the model to learn additional prior information.
- We propose a more efficient method for attention computation in image processing, which includes both channel attention and spatial attention. The channel attention is a multi-Dconv

head transposed attention and the spatial attention is a shifted windows-Dconv attention (SWDA).

- We present a more general approach by dividing the image into overlapping patches for independent inference, which improves the model performance.

2 Related Works

2.1 Image deblurring

The traditional deblurring algorithm typically involves formulating and solving an optimization problem based on the causes of image blurring [28, 64, 19, 55]. However, these approaches depend on manually designed image features, leading to limited generalization capability and constrained performance in intricate scenarios. Currently, deep learning-based on image deblurring focuses on establishing a direct mapping between blurred images and sharp images from paired datasets:

$$I_b = \phi(I_s; \theta_i), \quad (2)$$

where ϕ is the image blur function, and θ_i is a parameter vector. I_s is the sharp image. I_b is the blurred image. With the powerful fitting capability of deep learning, it is possible to directly train the model end-to-end to learn this mapping, thereby achieving deblurring [78, 41, 81]. Current research primarily focuses on general algorithms that aim to improve model representation by using advanced neural network architecture designs such as residual blocks, dense blocks, attention blocks, and others [75, 46, 44, 45, 24, 8, 15, 21, 33, 20]. Notably, the Transformer architecture [74, 17] has exhibited remarkable success. Numerous experiments have shown that the effectiveness of the Transformer primarily lies in the design of token mixer and the FFN(Feed-Forward Network) [79]. In particular, the self-attention mechanism in the token mixer is recognized as the key driver of its superior performance. However, its complexity increases quadratically as the number of patches grows, making it infeasible for high-resolution images. To address this issue, various revised token mixers [9, 3, 80, 72, 36, 76, 71, 30, 11] were developed to reduce complexity in different image processing applications. On the other side, different FFN designs such as Mlp [4], GluMlp [14], GatedMlp [48], ConvMlp [40] and SimpleGate [5] were proposed. While these designs have their own advantages and disadvantages in various low-level visual tasks, the performance difference remains consistent when the number of model parameters is nearly the same.

In addition to developing general algorithms, another focus is on creating specialized models optimized for specific blurry situations, including image super-resolution (SR), real-world image deblurring, image denoising, and the reduction of JPEG compression artifacts [22, 84, 42, 7, 32].

2.2 Diffusion Model

Recently, Diffusion Models have emerged as leaders in unconditional image synthesis, leveraging unsupervised learning algorithms to extract priors from datasets and achieve state-of-the-art results. In contrast to previous, models such as feed-forward, GAN, and flow-based models, which directly learn a mapping of f from the input x to the result y :

$$y = f(x), \quad (3)$$

The diffusion model adopts a distinct approach. It treats the generation process as an optimization computation, expressed as:

$$y = \arg \min_y E_\theta(x, y), \quad (4)$$

where E is the expectation and θ represents the parameters. The information it directly learns is not the joint distribution of pixels, but rather the gradient of the distribution. In other words, instead of learning a map directly, DM builds a neural network to find a solution to the optimization problem and then samples the solution to get an image.

Drawing upon its robust ability to grasp image priors from datasets, various impressive diffusion frameworks have been utilized for low-level vision tasks [52, 57, 31, 60, 26, 68, 16, 59, 18]. Nonetheless, training a highly advanced diffusion model often demands expensive computing resources. To address this limitation, we propose to circumvent this drawback with our Swintormer approach.

Table 1: Quantitative comparison by applying diffusion model [59] on the DPDD Dataset [1]. In order to make a fair comparison with other existing methods, the input image is an 8-bit image instead of a 16-bit image.

Model	PSNR \uparrow	SSIM \uparrow	MAE \downarrow	LPIPS \downarrow
Input	23.70	0.713	0.048	0.354
JNB [64]	23.69	0.707	0.048	0.442
EBDB [28]	23.94	0.723	0.047	0.402
DMENet [37]	23.90	0.720	0.047	0.410
Diffusion	23.94	0.727	0.047	0.349

3 Method

Our goal is to develop an image deblurring model that efficiently utilizes priors generated by the diffusion model while maintaining the advantage of being memory-efficient. We propose Sliding Window Image Restoration Model (Swintormer). The Swintormer is a regression-based model designed with a sliding window strategy. An overview of the pipeline is presented in Fig. 1. In this section, we introduce the design of the transform module in the model and demonstrate how diffusion is employed to generate prior features.

3.1 Shifted Windows-Dconv Attention

While self-attention [74, 17] is highly effective, the time and memory complexity of the key-query dot-product interaction grows quadratically in self-attention as the input resolution increases. For example, performing a calculation on a tensor of size $8 \times 128 \times 128 \times 48$ requires 64GB of video memory. Similar to deal with long sentence problems in NLP [9, 3, 80, 72, 36, 76, 71, 30, 11], many methods [43, 81, 5] are proposed for high-resolution image. However, these methods have different performance in different low-level visual tasks. Therefore, we propose Swintormer for improving generalization performance, that has linear complexity. The key innovation is to segment the feature tensor along the channel dimension and then calculate channel attention and spatial attention separately. Another crucial aspect is the use of depth-wise convolutions to generate *query* (\mathbf{Q}), *key* (\mathbf{K}) and *value* (\mathbf{V}) projections instead of using linear layers, which can highlight the local context to accelerate model convergence.

Given a layer normalized tensor $\mathbf{Y} \in \mathbb{R}^{\hat{H} \times \hat{W} \times \hat{C}}$, our SWDA first applies a shifted window partitioning approach to divide \mathbf{Y} into $M \times M$ patches (with a default window size of 16). One challenge with this routine is that some windows may end up smaller than $M \times M$. Therefore, a cyclic-shifting toward the top-left direction method is used to solve the problem [49]. The resulting patches are then used to generate \mathbf{Q} , \mathbf{K} and \mathbf{V} projections through 1×1 convolutions to aggregate pixel-wise cross-channel context, followed by 3×3 depth-wise bias-free convolutions. As a result, the tensors \mathbf{Q} , \mathbf{K} and \mathbf{V} are all the same size, $\mathbb{R}^{M \times M \times \hat{C}}$. These tensors are then split into two parts along the channel, each with a size of $\mathbb{R}^{M \times M \times \frac{\hat{C}}{2}}$. One part is used for channel attention calculation by MDTA [81], where their dot-product interaction produces a transposed-attention map of size $\mathbb{R}^{\frac{\hat{C}}{2} \times \frac{\hat{C}}{2}}$, while the other part is utilized for spatial attention calculation, resulting in an attention map with size of $\mathbb{R}^{M \times M}$. Overall, the process is defined as:

$$\text{Channel Attention} = \text{SoftMax}(Q_c K_c^T) V_c, \quad (5)$$

$$\text{Spacial Attention} = \text{SoftMax}(Q_s K_s^T + B) V_s, \quad (6)$$

$$\text{Attention} = W_p^{(\cdot)} \text{concat}(\text{Channel Attention}, \text{Spacial Attention}), \quad (7)$$

where $Q_c, K_c, V_c \in \mathbb{R}^{\frac{\hat{C}}{2} \times M^2}$; $Q_s, K_s, V_s \in \mathbb{R}^{M^2 \times \frac{\hat{C}}{2}}$; $B \in \mathbb{R}^{M^2 \times M^2}$ represents the relative position bias term for each head; $W_p^{(\cdot)}$ denotes the 1×1 point-wise convolution, and M^2 is the number of patches in a window. The relative position bias encodes the relative spatial configurations of visual elements.

3.2 Diffusion Model

Many methods, such as Masked Autoencoders [25], improve the performance of the model by destroying the feature and then rebuilding the feature. Based on this idea of the feature destruction

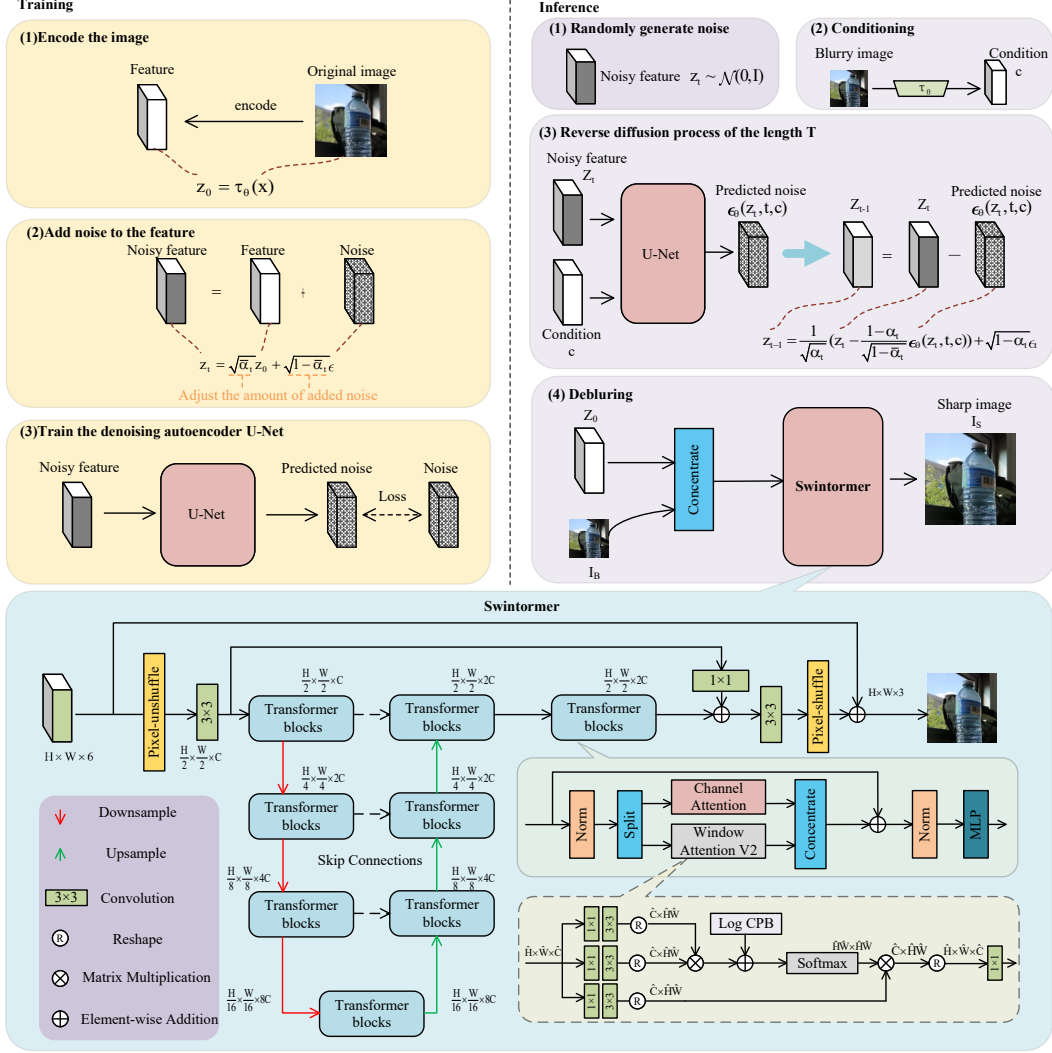


Figure 1: The architecture of the Swintormer.

and reconstruction, we introduce the diffusion model to process some important features. Specifically, our diffusion model is based on latent conditional denoising diffusion probabilistic models [59, 26]. It consists of a forward diffusion process $q(z_{1:T}|z_0)$ and a reverse denoising process $p_\theta(z_{0:T})$ where T is a fixed Markov Chain of length. When given a feature x , we use VQGAN [18] to obtain the latent space $z = \mathcal{E}(x)$. With the latent space, we compute the forward diffusion process for training the diffusion model and calculate the reverse denoising process for generating the processed feature.

Forward diffusion process. In the forward process, we input z and gradually add Gaussian noise \mathcal{N} to it according to a variance schedule β_1, \dots, β_T :

$$q(z_{1:T}|z_0) := \prod_{t=1}^T q(z_t|z_{t-1}), \quad (8)$$

$$q(z_t|z_{t-1}) := \mathcal{N}(z_t; \sqrt{1 - \beta_t}z_{t-1}, \beta_t \mathbf{I}) \quad (9)$$

By fixing the variances β_t to constants and the reparameterization [34] $z_t(z_0, \epsilon) = \sqrt{\alpha_t}z_0 + \sqrt{1 - \alpha_t}\epsilon$, for $\epsilon \sim \mathcal{N}(\mathbf{0}, \mathbf{I})$, thus Eq. (9) can be rewritten as:

$$q(z_t|z_0) = \mathcal{N}(z_t; \sqrt{\alpha_t}z_0, (1 - \alpha_t)\mathbf{I}) \quad (10)$$

where $\alpha_t := 1 - \beta_t$ and $\bar{\alpha}_t := \prod_{i=1}^t \alpha_i$. Specifically, we trained a denoising network ϵ_θ by predicting ϵ from z_t .

Reverse denoising process. In the reverse process $p_\theta(z_{0:T})$:

$$p_\theta(z_{0:T}) := p(z_T) \prod_{t=1}^T p_\theta(z_{t-1}|z_t), \quad (11)$$

$$p_\theta(z_{t-1}|z_t) := \mathcal{N}(z_{t-1}; \boldsymbol{\mu}_\theta(z_t, t), \boldsymbol{\Sigma}_\theta(z_t, t)) \quad (12)$$

Following previous work [26] to accelerate reverse processing by reparameterization, we generated the prior feature z_0 using KL divergence to directly compare $p_\theta(z_{0:T})$ against forward process posteriors from z_t to z_0 :

$$q(z_{t-1}|z_t, z_0) = \mathcal{N}(z_{t-1}; \tilde{\boldsymbol{\mu}}_t(z_t, z_0), \tilde{\beta}_t \mathbf{I}), \quad (13)$$

$$\text{where } \tilde{\boldsymbol{\mu}}_t(z_t, z_0) := \frac{\sqrt{\bar{\alpha}_{t-1}}\beta_t}{1 - \bar{\alpha}_t} z_0 + \frac{\sqrt{\bar{\alpha}_t}(1 - \bar{\alpha}_{t-1})}{1 - \bar{\alpha}_t} z_t, \quad (14)$$

$$\text{and } \tilde{\beta}_t := \frac{1 - \bar{\alpha}_{t-1}}{1 - \bar{\alpha}_t} \beta_t \quad (15)$$

Consequently, with the trained denoising network ϵ_θ conditioned on the c (The condition c is usually images [56], but can also be text and semantic maps [27, 58]) for predicting the noise ϵ , we can iteratively sample z_t as follows:

$$z_{t-1} = \frac{1}{\sqrt{\alpha_t}} \left(z_t - \frac{1 - \alpha_t}{\sqrt{1 - \bar{\alpha}_t}} \epsilon_\theta(z_t, t, c) \right) + \sqrt{1 - \alpha_t} \epsilon_t \quad (16)$$

where $\epsilon_t \sim \mathcal{N}(\mathbf{0}, \mathbf{I})$. After T iterations, we can get feature z_0 as illustrated in Fig. 1. We further explore the iteration numbers T in Section 5.

3.3 Inference Strategy

We introduce a novel strategy to ensure consistency between the input tensor sizes used in both training and inference. This is achieved by incorporating a pre-processing operation that employs shifted windows before the inference step. While this pre-processing operation may introduce additional computational overhead as overlapping regions are redundantly processed by the entire model, it also increases parallelization due to maintaining the same batch size, thereby expediting the inference process. Moreover, this approach grants control over the size of the overlapping region by adjusting the sliding pace, allowing for a more nuanced trade-off between deblurring quality and inference speed in practical applications.

3.4 Training Strategy

First, it is aimed to establish a diffusion model for feature extraction, and then train Swintormer for deblurring. We utilize a super-resolution LDM [16] to execute the diffusion model. This specific LDM is chosen because its generated features align more closely with the input image’s own feature distribution, rather than integrating the overall feature distribution of other images in the training dataset. The super-resolution LDM consists of a denoising autoencoder ϵ_θ and a VQGAN model τ_θ . The VQGAN is a pre-trained model, and in our approach, regardless of the training or inference stage, its parameters are frozen, and we only need to train the denoising autoencoder ϵ_θ in the LDM. ϵ_θ is a time-conditioned U-Net denoising autoencoder [59, 60]. Specifically, we first use $\tau_\theta(x)$ to encode the input image and obtain the feature z_0 . Then in the latent space, we iteratively add Gaussian noise to the input feature z_0 to obtain the blurred feature z_t . During this diffusion process, we train the denoising autoencoder $\epsilon_\theta(z_t, t, c)$; $t = 1 \dots T$ to make its estimated noise consistent with the Gaussian noise we introduce:

$$L_{LDM} := \mathbb{E}_{\mathcal{E}(x), y, \epsilon \sim \mathcal{N}(0, I), t} \left[\|\epsilon - \epsilon_\theta(z_t, t, \tau_\theta(y))\|_2^2 \right], \quad (17)$$

Here, the input y is the blurred image used to guide the diffusion process.

After that, we proceed to train the Swintormer deblurring model. We utilize the trained denoising autoencoder model ϵ_θ to estimate the noise present in the blurred image. The estimated noise is then used through Eq. (16) to sample and acquire the prior feature z_0 . Subsequently, along with the corresponding blurred image, it is employed in the training of the Swintormer model ϕ_θ . This training process incorporates the utilization of L_1 loss and perceptual loss as Eq. (18) and Eq. (19):

$$\mathcal{L}_{deblur} = \|I_s - \phi_\theta(I_b, z_0)\|_1 \quad (18)$$

$$\mathcal{L}_{deblur} = \|VGG(I_s) - VGG(\phi_\theta(I_b, z_0))\|_2^2 \quad (19)$$

Here, ϕ_θ is the deblurring model Swintormer, and VGG is the associated feature extraction model [65] during the deblurring process. We will explain the performance difference between these two loss functions in Section 4.

3.5 Inference

Using the trained denoising autoencoder and Swintormer for deblurring involves two corresponding stages. First, prior feature extraction is performed. The blurred image $x \in \mathbb{R}^{H \times W \times 3}$ to be processed is fed into the denoising autoencoder ϵ_θ , and the resulting encoded result z_t is diffused through the DDIM [67] to obtain the prior feature $z_0 \in \mathbb{R}^{H \times W \times 3}$. It is worth noting that the prior feature z_0 will not be decoded by the VQGAN model τ_θ . Instead, along the channel dimension, z_0 is concatenated with x to form an extended feature tensor $x_f \in \mathbb{R}^{H \times W \times 6}$ for deblurring computation. To reduce the distribution shifts between training and inference, we partition the feature tensor into the overlapping patches, resulting in the input tensor denoted as $x_{input} \in \mathbb{R}^{M \times M \times C \times B}$. Here, M signifies the window size, B is the training batch size, and the dimensions of the input tensor. After processing by Swintormer, deblurred image patches $x_{dp} \in \mathbb{R}^{M \times M \times 3 \times B}$ are obtained. Finally, the resulting patches are merged into a complete deblurred image $x_{db} \in \mathbb{R}^{H \times W \times 3}$, where the overlapping regions are averaged to generate the corresponding value.

4 Experiments and Analysis

We evaluate the proposed Swintormer on benchmark datasets for two tasks: **(a)** defocus deblurring, and **(b)** single-image motion deblurring. More details about the datasets, training protocols, and extra visual outcomes are available in the technical appendices. In tables showing the performance of the evaluated methods, the top scores are **highlighted**.

Table 2: Single-image defocus deblurring results on the RealDOF dataset [38]. Our method outperforms existing baselines without extra training data.

Method	PSNR \uparrow	SSIM \uparrow	LPIPS \downarrow
DPDNet [1]	22.87	0.670	0.425
KPAC [66]	23.98	0.716	0.336
IFAN [38]	24.71	0.749	0.306
Restormer [81]	25.08	0.769	0.289
DRBNet [61]	25.75	0.771	0.257
Swintormer(ours)	25.83	0.772	0.257

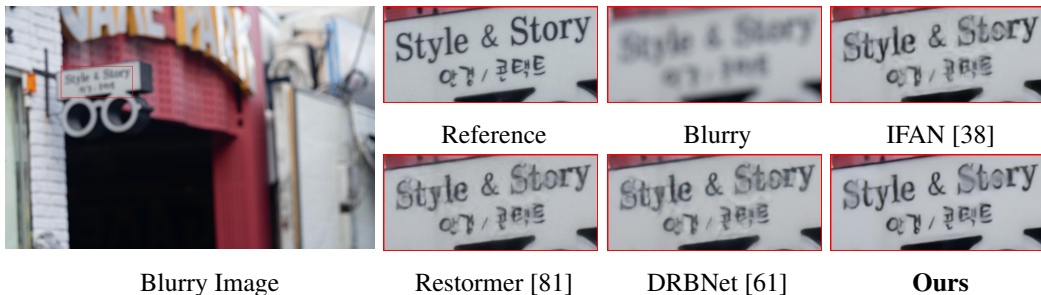


Figure 2: Visual comparison on the RealDOF dataset [38].

4.1 Defocus Deblurring Results

As shown in Table 2, our Swintormer performs best on the RealDOF dataset [38]. Table 3 shows image fidelity scores compared with conventional methods. Both version of our Swintormer trained under the two different loss functions have advantages compared with state-of-the-art. Particularly, in the outdoor scene category, Swintormer yields 0.12 dB improvements over the previous best method GRL [41]. And, it is worth noting that our method achieves the highest perceptual scores in terms of LPIPS on all scene categories.

Table 3: Deblurring results on the DPDD dataset(containing 37 indoor and 39 outdoor scenes). Swintormer sets new state-of-the-art in metric PSNR and LPIPS by using the L_1 loss function and the Perceptual loss function respectively. **S**: single-image defocus deblurring, **D**: dual-pixel defocus deblurring.

Method	Indoor Scenes				Outdoor Scenes				Combined			
	PSNR \uparrow	SSIM \uparrow	MAE \downarrow	LPIPS \downarrow	PSNR \uparrow	SSIM \uparrow	MAE \downarrow	LPIPS \downarrow	PSNR \uparrow	SSIM \uparrow	MAE \downarrow	LPIPS \downarrow
EBDB _S [28]	25.77	0.772	0.040	0.297	21.25	0.599	0.058	0.373	23.45	0.683	0.049	0.336
DMENet _S [37]	25.50	0.788	0.038	0.298	21.43	0.644	0.063	0.397	23.41	0.714	0.051	0.349
JNB _S [64]	26.73	0.828	0.031	0.273	21.10	0.608	0.064	0.355	23.84	0.715	0.048	0.315
DPDNet _S [1]	26.54	0.816	0.031	0.239	22.25	0.682	0.056	0.313	24.34	0.747	0.044	0.277
KPAC _S [66]	27.97	0.852	0.026	0.182	22.62	0.701	0.053	0.269	25.22	0.774	0.040	0.227
IFAN _S [38]	28.11	0.861	0.026	0.179	22.76	0.720	0.052	0.254	25.37	0.789	0.039	0.217
Restormer _S [81]	28.87	0.882	0.025	0.145	23.24	0.743	0.050	0.209	25.98	0.811	0.038	0.178
GRL _S [41]	29.06	0.886	0.024	0.139	23.45	0.761	0.049	0.196	26.18	0.822	0.037	0.168
Swintormer _S -Perceptual	28.95	0.883	0.025	0.141	23.33	0.750	0.050	0.205	26.09	0.819	0.038	0.168
Swintormer _S -L1	28.99	0.884	0.025	0.142	23.51	0.769	0.042	0.209	26.18	0.823	0.034	0.176
DPDNet _D [1]	27.48	0.849	0.029	0.189	22.90	0.726	0.052	0.255	25.13	0.786	0.041	0.223
RDPD _D [2]	28.10	0.843	0.027	0.210	22.82	0.704	0.053	0.298	25.39	0.772	0.040	0.255
Uformer _D [78]	28.23	0.860	0.026	0.199	23.10	0.728	0.051	0.285	25.65	0.795	0.039	0.243
IFAN _D [38]	28.66	0.868	0.025	0.172	23.46	0.743	0.049	0.240	25.99	0.804	0.037	0.207
Restormer _D [81]	29.48	0.895	0.023	0.134	23.97	0.773	0.047	0.175	26.66	0.833	0.035	0.155
GRL _D [41]	29.83	0.903	0.022	0.114	24.39	0.795	0.045	0.150	27.04	0.847	0.034	0.133
Swintormer _D -Perceptual	29.55	0.897	0.023	0.107	24.40	0.796	0.045	0.147	26.91	0.845	0.034	0.128
Swintormer _D -L1	29.74	0.899	0.022	0.127	24.52	0.798	0.045	0.167	27.07	0.847	0.034	0.148



Figure 3: Visual comparison on the DPDD dataset [1].

4.2 Motion Deblurring Results

Experimental results for motion deblurring are shown in Table 4. Our proposed method also achieved the leading performance.

Table 4: Single-image motion deblurring results on the GoPro dataset [54].

Method	MIMO-UNet [10]	HINet [6]	MAXIM [73]	Restormer [81]	UFormer [78]	DeepRFT [53]	MPRNet -local [12]	NAFNet [5]	GRL [41]	Swintormer ours
PSNR	32.68	32.71	32.86	32.92	32.97	33.23	33.31	33.69	33.93	33.38
SSIM	0.959	0.959	0.961	0.961	0.967	0.963	0.964	0.967	0.968	0.965

5 Ablation Studies

In this section, we investigate the effectiveness of the different designs of our proposed method. All experiments are conducted on the DPDD dataset. Previous findings have shown that our contributions have led to significant performance enhancements. Next, we will analyze the influence of each component individually.

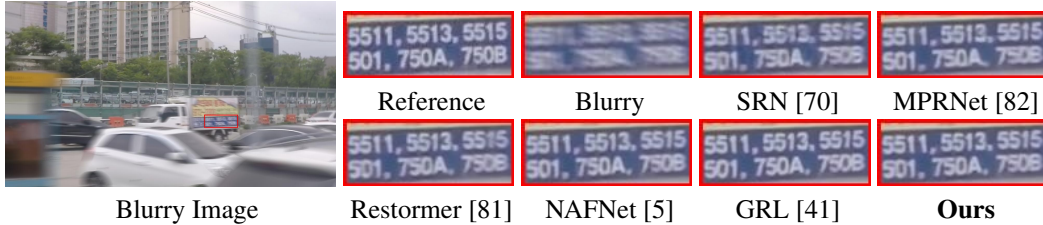


Figure 4: Visual comparison on the GoPro dataset [54].

Table 5: Ablation experiments. We train and test models on the DPDD dataset. For the baseline, we apply Restormer [81], a Transformer architecture based on channel attention(MDTA). T represents the iteration numbers in the diffusion model.

Network	Component	Params (M)	MACs (G)	PSNR (dB)
Baseline a	Transformer(MDTA)	25.05	1.93	26.66
Transformer block b	Transformer(Swin)	25.18	2.20	26.71
	Transformer(Swin+MDTA)	25.18	2.20	26.74
Pre-processing inference c	window size(256)+shift size(220)+Transformer(Swin+MDTA)	25.18	2.20	26.84
	window size(512)+shift size(220)+Transformer(Swin+MDTA)	25.18	2.20	26.98
	window size(512)+shift size(220)+Transformer(MDTA)	26.13	18.70	26.91
	window size(512)+shift size(384)+Transformer(Swin+MDTA)	25.18	2.20	26.89
Diffusion prior d	T(5)+Transformer(MDTA)	138.8	8.02	26.67
	T(10)+Transformer(MDTA)	138.8	8.02	26.71
	T(20)+Transformer(MDTA)	138.8	8.02	26.75
	T(50)+Transformer(MDTA)	138.8	8.02	26.77
Overall	T(50)+window size(512)+shift size(220)+Transformer(Swin+MDTA)	154.89	8.02	27.07

Improvements in mixed attention. Table 5b shows that the Shifted Windows-Dconv Attention has comparable performance with MDTA. Furthermore, introducing the Shifted Windows-Dconv Attention to MDTA brings a better performance. Overall, our proposed Transformer block contributions lead to a gain of 0.08 dB over the baseline.

Improvements in pre-processing inference. Table 5c shows that the pre-processing inference has comparable performance with TLC [13]. Furthermore, it’s noteworthy that a significant performance improvement of 0.25 dB over the baseline has been achieved by simply adjusting the window size and shift size to align the input tensor size with the training tensor size, without requiring retraining or fine-tuning.

Impact of diffusion prior. We construct a baseline model without priors generated by diffusion model. Table 5d demonstrates that the diffusion priors provide favorable gain of 0.11dB over the baseline. Furthermore, we explore the impact of the iteration numbers T in the diffusion model. A larger number of iterations leads the diffusion model to generate more accurate features. Therefore, the corresponding deblurring model can utilize the features more accurately. Based on testing results, when the number of iterations reaches 20, the improvement of the entire deblurring model gradually converges. However, for better performance, we choose $T = 50$ for the final model.

6 Conclusion

We endeavor to extend the applicability of deep learning deblurring methods beyond laboratory settings, aiming to achieve favorable results across a broader spectrum of real-world scenarios. Our principal contributions are presenting a new model and a new inference strategy that make deblur high-resolution images in personal computer possible. Specifically, integrated with DM, a memory-efficient model named Swintormer was built. It is an image deblurring Transformer model, designed to efficiently process high-resolution images with remarkably low MACs. The proposed Transformer block demonstrates improved performance by applying self-attention mechanisms across both channel and spatial dimensions, while maintaining linear complexity. Furthermore, we present a plug and play methodology that ensures consistency in input tensor sizes during training and inference, thereby enhancing model performance. Importantly, this approach obviates the need for retraining or fine-tuning, resulting in performance enhancements across various tasks.

References

- [1] Abuolaim, A., Brown, M.S.: Defocus deblurring using dual-pixel data. In: Vedaldi, A., Bischof, H., Brox, T., Frahm, J. (eds.) *Computer Vision - ECCV 2020 - 16th European Conference*, Glasgow, UK, August 23-28, 2020, Proceedings, Part X. *Lecture Notes in Computer Science*, vol. 12355, pp. 111–126. Springer (2020). https://doi.org/10.1007/978-3-030-58607-2_7, https://doi.org/10.1007/978-3-030-58607-2_7
- [2] Abuolaim, A., Delbracio, M., Kelly, D., Brown, M.S., Milanfar, P.: Learning to reduce defocus blur by realistically modeling dual-pixel data. In: *2021 IEEE/CVF International Conference on Computer Vision, ICCV 2021, Montreal, QC, Canada, October 10-17, 2021*. pp. 2269–2278. IEEE (2021). <https://doi.org/10.1109/ICCV48922.2021.00229>, <https://doi.org/10.1109/ICCV48922.2021.00229>
- [3] Beltagy, I., Peters, M.E., Cohan, A.: Longformer: The Long-Document Transformer. *ArXiv preprint **abs/2004.05150*** (2020), <https://arxiv.org/abs/2004.05150>
- [4] Burger, H.C., Schuler, C.J., Harmeling, S.: Image denoising: Can plain neural networks compete with bm3d? In: *2012 IEEE Conference on Computer Vision and Pattern Recognition*, Providence, RI, USA, June 16-21, 2012. pp. 2392–2399. IEEE Computer Society (2012). <https://doi.org/10.1109/CVPR.2012.6247952>, <https://doi.org/10.1109/CVPR.2012.6247952>
- [5] Chen, L., Chu, X., Zhang, X., Sun, J.: Simple baselines for image restoration. In: Avidan, S., Brostow, G.J., Cissé, M., Farinella, G.M., Hassner, T. (eds.) *Computer Vision - ECCV 2022 - 17th European Conference*, Tel Aviv, Israel, October 23-27, 2022, Proceedings, Part VII. *Lecture Notes in Computer Science*, vol. 13667, pp. 17–33. Springer (2022). https://doi.org/10.1007/978-3-031-20071-7_2, https://doi.org/10.1007/978-3-031-20071-7_2
- [6] Chen, L., Lu, X., Zhang, J., Chu, X., Chen, C.: Hinet: Half instance normalization network for image restoration. In: *IEEE Conference on Computer Vision and Pattern Recognition Workshops, CVPR Workshops 2021, virtual, June 19-25, 2021*. pp. 182–192. Computer Vision Foundation / IEEE (2021). <https://doi.org/10.1109/CVPRW53098.2021.00027>, https://openaccess.thecvf.com/content/CVPR2021W/NTIRE/html/Chen_HINet_Half_Instance_Normalization_Network_for_Image_Restoration_CVPRW_2021_paper.html
- [7] Chen, X., Wang, X., Zhou, J., Qiao, Y., Dong, C.: Activating more pixels in image super-resolution transformer. In: *Proceedings of the IEEE/CVF Conference on Computer Vision and Pattern Recognition (CVPR)*. pp. 22367–22377 (June 2023)
- [8] Cheng, W., Zhao, M., Ye, Z., Gu, S.: Mfagan: A compression framework for memory-efficient on-device super-resolution gan. *ArXiv preprint **abs/2107.12679*** (2021), <https://arxiv.org/abs/2107.12679>
- [9] Child, R., Gray, S., Radford, A., Sutskever, I.: Generating Long Sequences with Sparse Transformers. *ArXiv preprint **abs/1904.10509*** (2019), <https://arxiv.org/abs/1904.10509>
- [10] Cho, S., Ji, S., Hong, J., Jung, S., Ko, S.: Rethinking coarse-to-fine approach in single image deblurring. In: *2021 IEEE/CVF International Conference on Computer Vision, ICCV 2021, Montreal, QC, Canada, October 10-17, 2021*. pp. 4621–4630. IEEE (2021). <https://doi.org/10.1109/ICCV48922.2021.00460>, <https://doi.org/10.1109/ICCV48922.2021.00460>
- [11] Choromanski, K.M., Likhoshesterov, V., Dohan, D., Song, X., Gane, A., Sarlós, T., Hawkins, P., Davis, J.Q., Mohiuddin, A., Kaiser, L., Belanger, D.B., Colwell, L.J., Weller, A.: Rethinking attention with performers. In: *9th International Conference on Learning Representations, ICLR 2021, Virtual Event, Austria, May 3-7, 2021*. OpenReview.net (2021), <https://openreview.net/forum?id=Ua6zuk0WRH>
- [12] Chu, X., Chen, L., Chen, C., Lu, X.: Improving image restoration by revisiting global information aggregation. In: Avidan, S., Brostow, G.J., Cissé, M., Farinella, G.M., Hassner, T. (eds.) *Computer Vision - ECCV 2022 - 17th European Conference*, Tel Aviv, Israel, October 23-27, 2022, Proceedings, Part VII. *Lecture Notes in Computer Science*, vol. 13667, pp. 53–71. Springer (2022). https://doi.org/10.1007/978-3-031-20071-7_4, https://doi.org/10.1007/978-3-031-20071-7_4

- [13] Chu, X., Chen, L., Chen, C., Lu, X.: Improving image restoration by revisiting global information aggregation. In: Avidan, S., Brostow, G.J., Cissé, M., Farinella, G.M., Hassner, T. (eds.) *Computer Vision - ECCV 2022 - 17th European Conference*, Tel Aviv, Israel, October 23-27, 2022, Proceedings, Part VII. *Lecture Notes in Computer Science*, vol. 13667, pp. 53–71. Springer (2022). https://doi.org/10.1007/978-3-031-20071-7_4, https://doi.org/10.1007/978-3-031-20071-7_4
- [14] Dauphin, Y.N., Fan, A., Auli, M., Grangier, D.: Language modeling with gated convolutional networks. In: Precup, D., Teh, Y.W. (eds.) *Proceedings of the 34th International Conference on Machine Learning, ICML 2017, Sydney, NSW, Australia, 6-11 August 2017*. *Proceedings of Machine Learning Research*, vol. 70, pp. 933–941. PMLR (2017), <http://proceedings.mlr.press/v70/dauphin17a.html>
- [15] Deng, X., Zhang, Y., Xu, M., Gu, S., Duan, Y.: Deep coupled feedback network for joint exposure fusion and image super-resolution. *IEEE Transactions on Image Processing* **30**, 3098–3112 (2021)
- [16] Dhariwal, P., Nichol, A.Q.: Diffusion models beat gans on image synthesis. In: Ranzato, M., Beygelzimer, A., Dauphin, Y.N., Liang, P., Vaughan, J.W. (eds.) *Advances in Neural Information Processing Systems 34: Annual Conference on Neural Information Processing Systems 2021, NeurIPS 2021, December 6-14, 2021, virtual*. pp. 8780–8794 (2021), <https://proceedings.neurips.cc/paper/2021/hash/49ad23d1ec9fa4bd8d77d02681df5cfa-Abstract.html>
- [17] Dosovitskiy, A., Beyer, L., Kolesnikov, A., Weissenborn, D., Zhai, X., Unterthiner, T., Dehghani, M., Minderer, M., Heigold, G., Gelly, S., Uszkoreit, J., Houlsby, N.: An image is worth 16x16 words: Transformers for image recognition at scale. In: *9th International Conference on Learning Representations, ICLR 2021, Virtual Event, Austria, May 3-7, 2021*. OpenReview.net (2021), <https://openreview.net/forum?id=YicbFdNTTy>
- [18] Esser, P., Rombach, R., Ommer, B.: Taming transformers for high-resolution image synthesis. In: *IEEE Conference on Computer Vision and Pattern Recognition, CVPR 2021, virtual, June 19-25, 2021*. pp. 12873–12883. Computer Vision Foundation / IEEE (2021). <https://doi.org/10.1109/CVPR46437.2021.01268>, https://openaccess.thecvf.com/content/CVPR2021/html/Esser_Taming_Transformers_for_High-Resolution_Image_Synthesis_CVPR_2021_paper.html
- [19] Fergus, R., Singh, B., Hertzmann, A., Roweis, S.T., Freeman, W.T.: Removing camera shake from a single photograph. In: *ACM SIGGRAPH 2006 Papers*. p. 787–794. SIGGRAPH '06, Association for Computing Machinery, New York, NY, USA (2006). <https://doi.org/10.1145/1179352.1141956>, <https://doi.org/10.1145/1179352.1141956>
- [20] Fu, X., Wang, M., Cao, X., Ding, X., Zha, Z.J.: A model-driven deep unfolding method for jpeg artifacts removal. *IEEE Transactions on Neural Networks and Learning Systems* (2021)
- [21] Fu, X., Zha, Z., Wu, F., Ding, X., Paisley, J.W.: JPEG artifacts reduction via deep convolutional sparse coding. In: *2019 IEEE/CVF International Conference on Computer Vision, ICCV 2019, Seoul, Korea (South), October 27 - November 2, 2019*. pp. 2501–2510. IEEE (2019). <https://doi.org/10.1109/ICCV.2019.00259>, <https://doi.org/10.1109/ICCV.2019.00259>
- [22] Ghahremani, M., Khateri, M., Sierra, A., Tohka, J.: Adversarial distortion learning for medical image denoising. *ArXiv preprint [abs/2204.14100](https://arxiv.org/abs/2204.14100)* (2022), <https://arxiv.org/abs/2204.14100>
- [23] Goodfellow, I.J., Pouget-Abadie, J., Mirza, M., Xu, B., Warde-Farley, D., Ozair, S., Courville, A., Bengio, Y.: *Generative adversarial networks* (2014)
- [24] Guo, Y., Chen, J., Wang, J., Chen, Q., Cao, J., Deng, Z., Xu, Y., Tan, M.: Closed-loop matters: Dual regression networks for single image super-resolution. In: *2020 IEEE/CVF Conference on Computer Vision and Pattern Recognition, CVPR 2020, Seattle, WA, USA, June 13-19, 2020*. pp. 5406–5415. Computer Vision Foundation / IEEE (2020). <https://doi.org/10.1109/CVPR42600.2020.00545>, https://openaccess.thecvf.com/content_CVPR_2020/html/Guo_Closed-Loop_Matters_Dual_Regression_Networks_for_Single_Image_Super-Resolution_CVPR_2020_paper.html
- [25] He, K., Chen, X., Xie, S., Li, Y., Dollár, P., Girshick, R.B.: Masked autoencoders are scalable vision learners. In: *IEEE/CVF Conference on Computer Vision and Pattern Recognition*,

- CVPR 2022, New Orleans, LA, USA, June 18-24, 2022. pp. 15979–15988. IEEE (2022). <https://doi.org/10.1109/CVPR52688.2022.01553>, <https://doi.org/10.1109/CVPR52688.2022.01553>
- [26] Ho, J., Jain, A., Abbeel, P.: Denoising diffusion probabilistic models. In: Larochelle, H., Ranzato, M., Hadsell, R., Balcan, M., Lin, H. (eds.) *Advances in Neural Information Processing Systems 33: Annual Conference on Neural Information Processing Systems 2020, NeurIPS 2020, December 6-12, 2020, virtual (2020)*, <https://proceedings.neurips.cc/paper/2020/hash/4c5bcfec8584af0d967f1ab10179ca4b-Abstract.html>
- [27] Isola, P., Zhu, J., Zhou, T., Efros, A.A.: Image-to-image translation with conditional adversarial networks. In: *2017 IEEE Conference on Computer Vision and Pattern Recognition, CVPR 2017, Honolulu, HI, USA, July 21-26, 2017*. pp. 5967–5976. IEEE Computer Society (2017). <https://doi.org/10.1109/CVPR.2017.632>, <https://doi.org/10.1109/CVPR.2017.632>
- [28] Karaali, A., Jung, C.R.: Edge-based defocus blur estimation with adaptive scale selection. *TIP* (2017)
- [29] Karras, T., Laine, S., Aittala, M., Hellsten, J., Lehtinen, J., Aila, T.: Analyzing and improving the image quality of stylegan. In: *2020 IEEE/CVF Conference on Computer Vision and Pattern Recognition, CVPR 2020, Seattle, WA, USA, June 13-19, 2020*. pp. 8107–8116. Computer Vision Foundation / IEEE (2020). <https://doi.org/10.1109/CVPR42600.2020.00813>, https://openaccess.thecvf.com/content_CVPR_2020/html/Karras_Analyzing_and_Improving_the_Image_Quality_of_StyleGAN_CVPR_2020_paper.html
- [30] Katharopoulos, A., Vyas, A., Pappas, N., Fleuret, F.: Transformers are rnns: Fast autoregressive transformers with linear attention. In: *Proceedings of the 37th International Conference on Machine Learning, ICML 2020, 13-18 July 2020, Virtual Event. Proceedings of Machine Learning Research*, vol. 119, pp. 5156–5165. PMLR (2020), <http://proceedings.mlr.press/v119/katharopoulos20a.html>
- [31] Kwar, B., Elad, M., Ermon, S., Song, J.: Denoising diffusion restoration models. In: *Advances in Neural Information Processing Systems (2022)*
- [32] Kwar, B., Song, J., Ermon, S., Elad, M.: Jpeg artifact correction using denoising diffusion restoration models. In: *Neural Information Processing Systems (NeurIPS) Workshop on Score-Based Methods (2022)*
- [33] Kim, Y., Soh, J.W., Park, J., Ahn, B., Lee, H.S., Moon, Y.S., Cho, N.I.: A pseudo-blind convolutional neural network for the reduction of compression artifacts. *IEEE Transactions on Circuits and Systems for Video Technology* **30**(4), 1121–1135 (2019)
- [34] Kingma, D.P., Welling, M.: Auto-encoding variational bayes. In: Bengio, Y., LeCun, Y. (eds.) *2nd International Conference on Learning Representations, ICLR 2014, Banff, AB, Canada, April 14-16, 2014, Conference Track Proceedings (2014)*, <http://arxiv.org/abs/1312.6114>
- [35] Kingma, D.P., Welling, M.: Auto-encoding variational bayes (2022)
- [36] Kitaev, N., Kaiser, L., Levskaya, A.: Reformer: The efficient transformer. In: *8th International Conference on Learning Representations, ICLR 2020, Addis Ababa, Ethiopia, April 26-30, 2020. OpenReview.net (2020)*, <https://openreview.net/forum?id=rkgNkkHtvB>
- [37] Lee, J., Lee, S., Cho, S., Lee, S.: Deep defocus map estimation using domain adaptation. In: *IEEE Conference on Computer Vision and Pattern Recognition, CVPR 2019, Long Beach, CA, USA, June 16-20, 2019*. pp. 12222–12230. Computer Vision Foundation / IEEE (2019). <https://doi.org/10.1109/CVPR.2019.01250>, http://openaccess.thecvf.com/content_CVPR_2019/html/Lee_Deep_Defocus_Map_Estimation_Using_Domain_Adaptation_CVPR_2019_paper.html
- [38] Lee, J., Son, H., Rim, J., Cho, S., Lee, S.: Iterative filter adaptive network for single image defocus deblurring. In: *IEEE Conference on Computer Vision and Pattern Recognition, CVPR 2021, virtual, June 19-25, 2021*. pp. 2034–2042. Computer Vision Foundation / IEEE (2021). <https://doi.org/10.1109/CVPR46437.2021.00207>, https://openaccess.thecvf.com/content/CVPR2021/html/Lee_Iterative_Filter_Adaptive_Network_for_Single_Image_Defocus_Deblurring_CVPR_2021_paper.html

- [39] Lempitsky, V., Vedaldi, A., Ulyanov, D.: Deep image prior. In: 2018 IEEE/CVF Conference on Computer Vision and Pattern Recognition. pp. 9446–9454 (2018). <https://doi.org/10.1109/CVPR.2018.00984>
- [40] Li, J., Hassani, A., Walton, S., Shi, H.: Convmlp: Hierarchical convolutional mlps for vision. In: IEEE/CVF Conference on Computer Vision and Pattern Recognition, CVPR 2023 - Workshops, Vancouver, BC, Canada, June 17-24, 2023. pp. 6307–6316. IEEE (2023). <https://doi.org/10.1109/CVPRW59228.2023.00671>, <https://doi.org/10.1109/CVPRW59228.2023.00671>
- [41] Li, Y., Fan, Y., Xiang, X., Demandolx, D., Ranjan, R., Timofte, R., Gool, L.V.: Efficient and explicit modelling of image hierarchies for image restoration. In: IEEE/CVF Conference on Computer Vision and Pattern Recognition, CVPR 2023, Vancouver, BC, Canada, June 17-24, 2023. pp. 18278–18289. IEEE (2023). <https://doi.org/10.1109/CVPR52729.2023.01753>, <https://doi.org/10.1109/CVPR52729.2023.01753>
- [42] Liang, J., Cao, J., Sun, G., Zhang, K., Gool, L.V., Timofte, R.: Swinir: Image restoration using swin transformer. In: IEEE/CVF International Conference on Computer Vision Workshops, ICCVW 2021, Montreal, BC, Canada, October 11-17, 2021. pp. 1833–1844. IEEE (2021). <https://doi.org/10.1109/ICCVW54120.2021.00210>, <https://doi.org/10.1109/ICCVW54120.2021.00210>
- [43] Liang, J., Cao, J., Sun, G., Zhang, K., Gool, L.V., Timofte, R.: Swinir: Image restoration using swin transformer. In: IEEE/CVF International Conference on Computer Vision Workshops, ICCVW 2021, Montreal, BC, Canada, October 11-17, 2021. pp. 1833–1844. IEEE (2021). <https://doi.org/10.1109/ICCVW54120.2021.00210>, <https://doi.org/10.1109/ICCVW54120.2021.00210>
- [44] Liang, J., Lugmayr, A., Zhang, K., Danelljan, M., Gool, L.V., Timofte, R.: Hierarchical conditional flow: A unified framework for image super-resolution and image rescaling. In: 2021 IEEE/CVF International Conference on Computer Vision, ICCV 2021, Montreal, QC, Canada, October 10-17, 2021. pp. 4056–4065. IEEE (2021). <https://doi.org/10.1109/ICCV48922.2021.00404>, <https://doi.org/10.1109/ICCV48922.2021.00404>
- [45] Liang, J., Sun, G., Zhang, K., Gool, L.V., Timofte, R.: Mutual affine network for spatially variant kernel estimation in blind image super-resolution. In: 2021 IEEE/CVF International Conference on Computer Vision, ICCV 2021, Montreal, QC, Canada, October 10-17, 2021. pp. 4076–4085. IEEE (2021). <https://doi.org/10.1109/ICCV48922.2021.00406>, <https://doi.org/10.1109/ICCV48922.2021.00406>
- [46] Liang, J., Zhang, K., Gu, S., Gool, L.V., Timofte, R.: Flow-based kernel prior with application to blind super-resolution. In: IEEE Conference on Computer Vision and Pattern Recognition, CVPR 2021, virtual, June 19-25, 2021. pp. 10601–10610. Computer Vision Foundation / IEEE (2021). <https://doi.org/10.1109/CVPR46437.2021.01046>, https://openaccess.thecvf.com/content/CVPR2021/html/Liang_Flow-Based_Kernel_Prior_With_Application_to_Blind_Super-Resolution_CVPR_2021_paper.html
- [47] Lin, T.Y., Maire, M., Belongie, S., Bourdev, L., Girshick, R., Hays, J., Perona, P., Ramanan, D., Zitnick, C.L., Dollár, P.: Microsoft coco: Common objects in context (2015)
- [48] Liu, H., Dai, Z., So, D.R., Le, Q.V.: Pay attention to mlps. In: Ranzato, M., Beygelzimer, A., Dauphin, Y.N., Liang, P., Vaughan, J.W. (eds.) Advances in Neural Information Processing Systems 34: Annual Conference on Neural Information Processing Systems 2021, NeurIPS 2021, December 6-14, 2021, virtual. pp. 9204–9215 (2021), <https://proceedings.neurips.cc/paper/2021/hash/4cc05b35c2f937c5bd9e7d41d3686fff-Abstract.html>
- [49] Liu, Z., Lin, Y., Cao, Y., Hu, H., Wei, Y., Zhang, Z., Lin, S., Guo, B.: Swin transformer: Hierarchical vision transformer using shifted windows. In: 2021 IEEE/CVF International Conference on Computer Vision, ICCV 2021, Montreal, QC, Canada, October 10-17, 2021. pp. 9992–10002. IEEE (2021). <https://doi.org/10.1109/ICCV48922.2021.00986>, <https://doi.org/10.1109/ICCV48922.2021.00986>
- [50] Loshchilov, I., Hutter, F.: SGDR: stochastic gradient descent with warm restarts. In: 5th International Conference on Learning Representations, ICLR 2017, Toulon, France, April 24-26, 2017, Conference Track Proceedings. OpenReview.net (2017), <https://openreview.net/forum?id=Skq89Scxx>

- [51] Loshchilov, I., Hutter, F.: Decoupled weight decay regularization. In: International Conference on Learning Representations (2019), <https://openreview.net/forum?id=Bkg6RiCqY7>
- [52] Luo, Z., Gustafsson, F.K., Zhao, Z., Sjölund, J., Schön, T.B.: Image restoration with mean-reverting stochastic differential equations. International Conference on Machine Learning (2023)
- [53] Mao, X., Liu, Y., Shen, W., Li, Q., Wang, Y.: Deep residual fourier transformation for single image deblurring. ArXiv preprint **abs/2111.11745** (2021), <https://arxiv.org/abs/2111.11745>
- [54] Nah, S., Kim, T.H., Lee, K.M.: Deep multi-scale convolutional neural network for dynamic scene deblurring. In: 2017 IEEE Conference on Computer Vision and Pattern Recognition, CVPR 2017, Honolulu, HI, USA, July 21-26, 2017. pp. 257–265. IEEE Computer Society (2017). <https://doi.org/10.1109/CVPR.2017.35>, <https://doi.org/10.1109/CVPR.2017.35>
- [55] Pan, J., Sun, D., Pfister, H., Yang, M.H.: Deblurring images via dark channel prior. IEEE Transactions on Pattern Analysis and Machine Intelligence **40**(10), 2315–2328 (2018). <https://doi.org/10.1109/TPAMI.2017.2753804>
- [56] Park, T., Liu, M., Wang, T., Zhu, J.: Semantic image synthesis with spatially-adaptive normalization. In: IEEE Conference on Computer Vision and Pattern Recognition, CVPR 2019, Long Beach, CA, USA, June 16-20, 2019. pp. 2337–2346. Computer Vision Foundation / IEEE (2019). <https://doi.org/10.1109/CVPR.2019.00244>, http://openaccess.thecvf.com/content_CVPR_2019/html/Park_Semantic_Image_Synthesis_With_Spatially-Adaptive_Normalization_CVPR_2019_paper.html
- [57] Peebles, W., Xie, S.: Scalable diffusion models with transformers (2023)
- [58] Reed, S.E., Akata, Z., Yan, X., Logeswaran, L., Schiele, B., Lee, H.: Generative adversarial text to image synthesis. In: Balcan, M., Weinberger, K.Q. (eds.) Proceedings of the 33rd International Conference on Machine Learning, ICML 2016, New York City, NY, USA, June 19-24, 2016. JMLR Workshop and Conference Proceedings, vol. 48, pp. 1060–1069. JMLR.org (2016), <http://proceedings.mlr.press/v48/reed16.html>
- [59] Rombach, R., Blattmann, A., Lorenz, D., Esser, P., Ommer, B.: High-resolution image synthesis with latent diffusion models. In: IEEE/CVF Conference on Computer Vision and Pattern Recognition, CVPR 2022, New Orleans, LA, USA, June 18-24, 2022. pp. 10674–10685. IEEE (2022). <https://doi.org/10.1109/CVPR52688.2022.01042>, <https://doi.org/10.1109/CVPR52688.2022.01042>
- [60] Ronneberger, O., Fischer, P., Brox, T.: U-net: Convolutional networks for biomedical image segmentation. In: MICCAI (3). Lecture Notes in Computer Science, vol. 9351, pp. 234–241. Springer (2015)
- [61] Ruan, L., Chen, B., Li, J., Lam, M.: Learning to deblur using light field generated and real defocus images. In: IEEE/CVF Conference on Computer Vision and Pattern Recognition, CVPR 2022, New Orleans, LA, USA, June 18-24, 2022. pp. 16283–16292. IEEE (2022). <https://doi.org/10.1109/CVPR52688.2022.01582>, <https://doi.org/10.1109/CVPR52688.2022.01582>
- [62] Russakovsky, O., Deng, J., Su, H., Krause, J., Satheesh, S., Ma, S., Huang, Z., Karpathy, A., Khosla, A., Bernstein, M., Berg, A.C., Fei-Fei, L.: Imagenet large scale visual recognition challenge (2015)
- [63] Schuler, C.J., Hirsch, M., Harmeling, S., Schölkopf, B.: Learning to deblur. IEEE Transactions on Pattern Analysis and Machine Intelligence **38**(7), 1439–1451 (2016). <https://doi.org/10.1109/TPAMI.2015.2481418>
- [64] Shi, J., Xu, L., Jia, J.: Just noticeable defocus blur detection and estimation. In: IEEE Conference on Computer Vision and Pattern Recognition, CVPR 2015, Boston, MA, USA, June 7-12, 2015. pp. 657–665. IEEE Computer Society (2015). <https://doi.org/10.1109/CVPR.2015.7298665>, <https://doi.org/10.1109/CVPR.2015.7298665>
- [65] Simonyan, K., Zisserman, A.: Very deep convolutional networks for large-scale image recognition. In: Bengio, Y., LeCun, Y. (eds.) 3rd International Conference on Learning Representations, ICLR 2015, San Diego, CA, USA, May 7-9, 2015, Conference Track Proceedings (2015), <http://arxiv.org/abs/1409.1556>

- [66] Son, H., Lee, J., Cho, S., Lee, S.: Single image defocus deblurring using kernel-sharing parallel atrous convolutions. In: 2021 IEEE/CVF International Conference on Computer Vision, ICCV 2021, Montreal, QC, Canada, October 10-17, 2021. pp. 2622–2630. IEEE (2021). <https://doi.org/10.1109/ICCV48922.2021.00264>, <https://doi.org/10.1109/ICCV48922.2021.00264>
- [67] Song, J., Meng, C., Ermon, S.: Denoising diffusion implicit models. arXiv:2010.02502 (October 2020), <https://arxiv.org/abs/2010.02502>
- [68] Song, Y., Sohl-Dickstein, J., Kingma, D.P., Kumar, A., Ermon, S., Poole, B.: Score-based generative modeling through stochastic differential equations. In: 9th International Conference on Learning Representations, ICLR 2021, Virtual Event, Austria, May 3-7, 2021. OpenReview.net (2021), <https://openreview.net/forum?id=PXTIG12RRHS>
- [69] Swofford, M.: Image completion on cifar-10 (2018)
- [70] Tao, X., Gao, H., Shen, X., Wang, J., Jia, J.: Scale-recurrent network for deep image deblurring. In: IEEE Conference on Computer Vision and Pattern Recognition (CVPR) (2018)
- [71] Tay, Y., Bahri, D., Metzler, D., Juan, D.C., Zhao, Z., Zheng, C.: Synthesizer: Rethinking Self-Attention in Transformer Models. ArXiv preprint **abs/2005.00743** (2020), <https://arxiv.org/abs/2005.00743>
- [72] Tay, Y., Bahri, D., Yang, L., Metzler, D., Juan, D.: Sparse sinkhorn attention. In: Proceedings of the 37th International Conference on Machine Learning, ICML 2020, 13-18 July 2020, Virtual Event. Proceedings of Machine Learning Research, vol. 119, pp. 9438–9447. PMLR (2020), <http://proceedings.mlr.press/v119/tay20a.html>
- [73] Tu, Z., Talebi, H., Zhang, H., Yang, F., Milanfar, P., Bovik, A.C., Li, Y.: MAXIM: multi-axis MLP for image processing. In: IEEE/CVF Conference on Computer Vision and Pattern Recognition, CVPR 2022, New Orleans, LA, USA, June 18-24, 2022. pp. 5759–5770. IEEE (2022). <https://doi.org/10.1109/CVPR52688.2022.00568>, <https://doi.org/10.1109/CVPR52688.2022.00568>
- [74] Vaswani, A., Shazeer, N., Parmar, N., Uszkoreit, J., Jones, L., Gomez, A.N., Kaiser, L., Polosukhin, I.: Attention is all you need. In: Guyon, I., von Luxburg, U., Bengio, S., Wallach, H.M., Fergus, R., Vishwanathan, S.V.N., Garnett, R. (eds.) Advances in Neural Information Processing Systems 30: Annual Conference on Neural Information Processing Systems 2017, December 4-9, 2017, Long Beach, CA, USA. pp. 5998–6008 (2017), <https://proceedings.neurips.cc/paper/2017/hash/3f5ee243547dee91fbd053c1c4a845aa-Abstract.html>
- [75] Wang, L., Wang, Y., Lin, Z., Yang, J., An, W., Guo, Y.: Learning A single network for scale-arbitrary super-resolution. In: 2021 IEEE/CVF International Conference on Computer Vision, ICCV 2021, Montreal, QC, Canada, October 10-17, 2021. pp. 4781–4790. IEEE (2021). <https://doi.org/10.1109/ICCV48922.2021.00476>, <https://doi.org/10.1109/ICCV48922.2021.00476>
- [76] Wang, S., Li, B.Z., Khabsa, M., Fang, H., Ma, H.: Linformer: Self-Attention with Linear Complexity. ArXiv preprint **abs/2006.04768** (2020), <https://arxiv.org/abs/2006.04768>
- [77] Wang, X., Girshick, R.B., Gupta, A., He, K.: Non-local neural networks. In: 2018 IEEE Conference on Computer Vision and Pattern Recognition, CVPR 2018, Salt Lake City, UT, USA, June 18-22, 2018. pp. 7794–7803. Computer Vision Foundation / IEEE Computer Society (2018). <https://doi.org/10.1109/CVPR.2018.00813>, http://openaccess.thecvf.com/content_cvpr_2018/html/Wang_Non-Local_Neural_Networks_CVPR_2018_paper.html
- [78] Wang, Z., Cun, X., Bao, J., Zhou, W., Liu, J., Li, H.: Uformer: A general u-shaped transformer for image restoration. In: IEEE/CVF Conference on Computer Vision and Pattern Recognition, CVPR 2022, New Orleans, LA, USA, June 18-24, 2022. pp. 17662–17672. IEEE (2022). <https://doi.org/10.1109/CVPR52688.2022.01716>, <https://doi.org/10.1109/CVPR52688.2022.01716>
- [79] Yu, W., Luo, M., Zhou, P., Si, C., Zhou, Y., Wang, X., Feng, J., Yan, S.: Metaformer is actually what you need for vision. In: IEEE/CVF Conference on Computer Vision and Pattern Recognition, CVPR 2022, New Orleans, LA, USA, June 18-24, 2022. pp. 10809–10819. IEEE (2022). <https://doi.org/10.1109/CVPR52688.2022.01055>, <https://doi.org/10.1109/CVPR52688.2022.01055>

- [80] Zaheer, M., Guruganesh, G., Dubey, K.A., Ainslie, J., Alberti, C., Ontañón, S., Pham, P., Ravula, A., Wang, Q., Yang, L., Ahmed, A.: Big bird: Transformers for longer sequences. In: Larochelle, H., Ranzato, M., Hadsell, R., Balcan, M., Lin, H. (eds.) *Advances in Neural Information Processing Systems 33: Annual Conference on Neural Information Processing Systems 2020, NeurIPS 2020, December 6-12, 2020, virtual (2020)*, <https://proceedings.neurips.cc/paper/2020/hash/c8512d142a2d849725f31a9a7a361ab9-Abstract.html>
- [81] Zamir, S.W., Arora, A., Khan, S., Hayat, M., Khan, F.S., Yang, M.: Restormer: Efficient transformer for high-resolution image restoration. In: *IEEE/CVF Conference on Computer Vision and Pattern Recognition, CVPR 2022, New Orleans, LA, USA, June 18-24, 2022*. pp. 5718–5729. IEEE (2022). <https://doi.org/10.1109/CVPR52688.2022.00564>, <https://doi.org/10.1109/CVPR52688.2022.00564>
- [82] Zamir, S.W., Arora, A., Khan, S., Hayat, M., Khan, F.S., Yang, M.H., Shao, L.: Multi-stage progressive image restoration. In: *CVPR (2021)*
- [83] Zhang, H., Goodfellow, I.J., Metaxas, D.N., Odena, A.: Self-attention generative adversarial networks. In: Chaudhuri, K., Salakhutdinov, R. (eds.) *Proceedings of the 36th International Conference on Machine Learning, ICML 2019, 9-15 June 2019, Long Beach, California, USA. Proceedings of Machine Learning Research*, vol. 97, pp. 7354–7363. PMLR (2019), <http://proceedings.mlr.press/v97/zhang19d.html>
- [84] Zhang, Y., Li, D., Shi, X., He, D., Song, K., Wang, X., Qin, H., Li, H.: Kbnnet: Kernel basis network for image restoration. *ArXiv preprint **abs/2303.02881*** (2023), <https://arxiv.org/abs/2303.02881>